

# Computational fluid dynamics analysis of 1 MW steam turbine inlet geometries

ARKADIUSZ KOPROWSKI<sup>a,\*</sup>  
ROMUALD RZADKOWSKI<sup>a,b</sup>

<sup>a</sup> Institute of Fluid Flow Machinery Polish Academy of Sciences,  
Fiszera 14, 80-952 Gdańsk, Poland

<sup>b</sup> Air Force Institute of Technology, Księcia Bolesława, 6, 01-494 Warsaw,  
Poland

**Abstract** This paper analyses the influence of three different ring-type inlet duct geometries on the performance of a small 1 MW backpressure steam turbine. It examines the efficiency and pressure drop of seven turbine variants, including four spiral inlet geometries and three stages with a mass flow rate around 30 t/h. A one-pipe and two-pipe inlets are analysed from aerodynamical point of view, taking into account stator and rotor blades in three stages without the outlet. An outlet is added to the best variant. Also analysed is the occurrence of vortices in the inlets of the studied variants 1–7 as well as the efficiency, drop pressure, turbine power and mass flow. Finally, the best inlet for a 1 MW steam turbine is suggested.

**Keywords:** CFD analysis; Steam turbine; Inlet

## 1 Introduction

One of the main aims in designing a steam turbine is to increase its efficiency. This can be done by minimizing flow losses. The flow losses in the stator and rotor blades without an inlet chamber have been analysed in many papers, *e.g.* [1]. The inlet of a steam turbine generally consists of inlet boxes with partial admission together as well control and shut-off valves

---

\*Corresponding Author. Email: [akoprowski@imp.gda.pl](mailto:akoprowski@imp.gda.pl)

at the front of the turbine. Unsteady forces acting on rotor blades caused by partial admission are analysed in [1, 2].

In small turbines, the design of the inlet is simplified to lower production costs. Only a few analyses of the inlet chamber appear in the literature. Van den Braembussche shows that the flow angle distribution at the inlet chamber exit has to be uniform to ensure a high stator blade efficiency [3]. A large vortex around the rotor axis might appear if the inlet duct has no splitter plate installed. This large vortex leads to higher losses and an irregular mass flux distribution in front of the blade rows. Drexler proposes an evenly distributed mass flux upstream the stator blades to minimize mixing losses [4]. In order to reduce flow separation losses in the inlet chamber, Traupel [5] and Van den Braembussche [3] recommend maximizing the ratio between the inlet and outlet areas. Kovats argues that minimizing separated flow areas can reduce overall inlet losses by 30% [6]. Flow measurements in inlet ducts have been made by Lüdtke [7]. In the observed duct, two large vortices were detected opposite the radially arranged inlet pipe, which increased the losses. The inlet chamber of a double-flow low pressure turbine with one radially arranged inlet pipe was studied numerically by Sievert using computational fluid dynamics (CFD) simulations [8]. A swirling flow field was calculated within the inlet chamber resulting in increased pressure loss and high incidence angles in front of the stator rows. US patent [9] shows four pipe inlet chambers in a turbine. It also describes necessary changes of nozzle profiles.

Škach *et al.* [10] studied the design procedure of special stator blades for a single-pipe spiral inlet. Such inlets are used in high pressure and intermediate pressure steam turbines. The analysis showed improvement in steam flow uniformity and a reduction of aerodynamic losses in the blades. The spiral inlet calculations were analytical. The losses in inlet spiral, however, were not analysed. Hecker *et al.* [11] numerically analysed a ring-type inlet duct comprising two opposite pipes in one plane. The optimization of the inlet was carried out to minimize the loss of total pressure in the inlet duct and stator blades. The rotor and stator blades were not taken into account. Aerodynamic and mechanical analyses of the inlet and casing were done. Gao *et al.* [12] proposed a new type of 300 MW control stage inlet chamber which can reduce local aerodynamic exciting forces using 3D unsteady flow. This inlet chamber only has a slight influence on the overall performance.

Engelmann *et al.* [13] analysed the flow in T-junction pipes in order to calculate secondary losses. Presented was a numerical prediction of two typical steam admission branches: rotational symmetrical constructions with

spiral or circumferential slots and semi-detached branches. T-junction computations were used to determine additional secondary losses caused by steam admission.

This paper analyses the efficiency and pressure drop of seven steam turbine variants comprising three stages and four spiral inlet geometries that were designed to be around 1 MW with the flow around 30 t/h for the assumed inlet and outlet pressure values and the inlet temperature. Single-pipe and two-pipe inlets are analysed aerodynamically for the first time, taking into account the stator and rotor blades in three stages to find the best variant. The last variant includes turbine outlet together with a two-pipe inlet and three stator-rotor stages. The efficiency, pressure drop, turbine power and mass flow of all seven variants were analysed and compared.

## 2 Numerical analysis

The steady viscous calculations of the 3 inlets and 3 stages (32 stators and 99 rotor blades in each stage) was carried out using commercial, high-performance, general purpose computational fluid dynamics software Ansys CFX [16,20]. The geometry of the blades and turbine inlets and outlet was carried out using the Design Modeller [19]. The blade mesh was prepared in a commercial software Ansys TurboGrid [18] and the inlet in Ansys Meshing [17].

The inlet pressure was 900 kPa, temperature 493.15 K (220°C), and the outlet pressure was 400 kPa. The efficiency, pressure drop, turbine power and mass flow of all seven variants were analysed and compared.

### 2.1 Variant 1

In [10], an inlet spiral and inlet with circular cross-sections were analysed. Analysed here is a spiral inlet with a nearly rectangular cross-section and an inlet with a circular cross-section. The circular pipe is connected to the rectangular channel at a slight angle. The spiral outlet is shaped as a tapering ring (Fig. 1a) that leads the steam to stator blades. The rectangular channel is separated from the ending of the spiral by a wall (Fig. 1b). The inlet is oriented so that the flow is perpendicular to pressure side of the first stage stator blades and the angle of attack is below 90°. The profile of the first stator is S-9012A [14] and the number of the stators blades is 32.

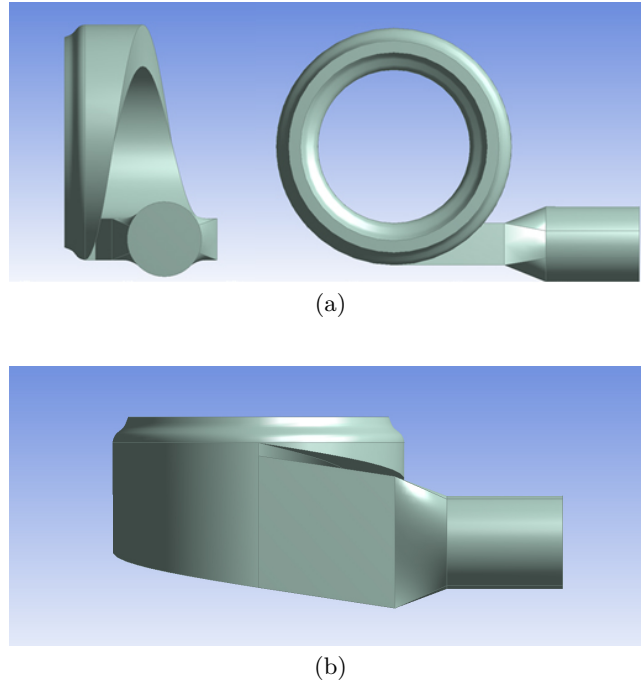


Figure 1: Variant 1 inlet geometry.

In Fig. 2, the distribution of total pressure in the tapered ring is shown. The distribution is not axisymmetric due to the separation of the inlet channel from the ending of the spiral and the asymmetry of the spiral. The maximal difference between total pressures is about 20 kPa.

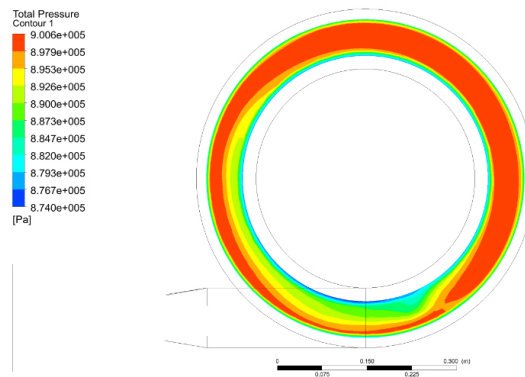


Figure 2: Total pressure in the inlet spiral, variant 1.

In order to locate the formation of the losses in the inlet geometry, the distribution of entropy was analyzed. As shown in Fig. 3 the entropy is highest at the end of the spiral, where it is separated by a wall (Fig. 1b). The high entropy values also occur near the inner wall of the spiral. These values reveal the presence of a vortex (see Fig. 4). Figure 4 also show that the pressure on the outer surface of the inlet is higher than on inner surface due to centrifugal forces.

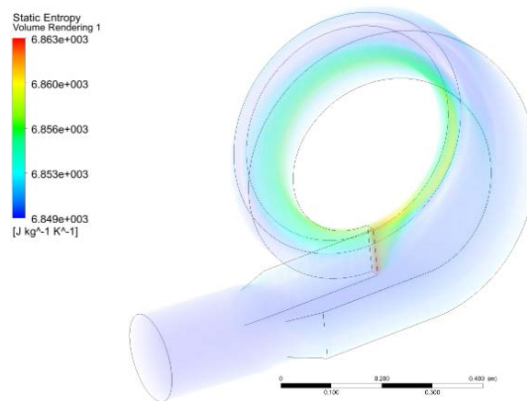


Figure 3: Entropy in inlet of variant 1.

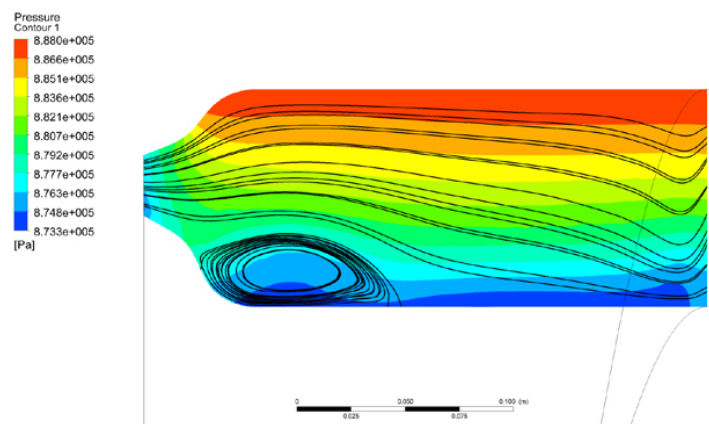


Figure 4: Pressure and streamlines in radial cross-section of variant 1 inlet spiral.

The flow in the turbine blades is presented in Fig. 5, which shows that the velocity is perpendicular to the pressure side of first stage stator blades.

This phenomenon in connection with the appearance of vortices in the inlet spiral (Fig. 4), lowers the efficiency to 86.17%. The turbine power was 1.368 MW and the mass flow 9.78 kg/s (35.21 t/h). The pressure drop in the inlet was 5.64 kPa as a result of friction loss and local losses.

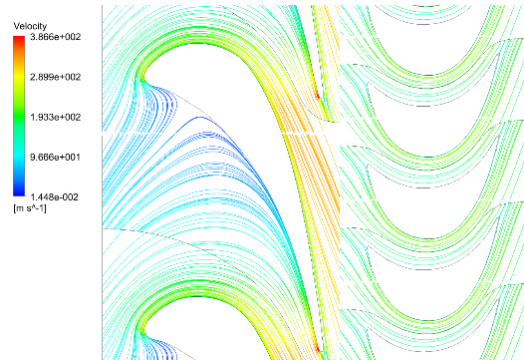


Figure 5: Velocity field in 0.5 length stator blade, variant 1.

## 2.2 Variant 2

Variant 2 had the same inlet spiral geometry as variant 1, but a different first stator profile (S-5515A [14]), which was introduced in order to prevent the flow from being perpendicular to the pressure side of the 1st stage stator blades. Additionally, the number of the stator blades was changed to 39. These changes did not noticeably alter the inlet flow. The pressure distribution and streamlines shapes were almost identical to those of variant 1 (Figs. 6 and 7). However, the new stator blade profiles increased the

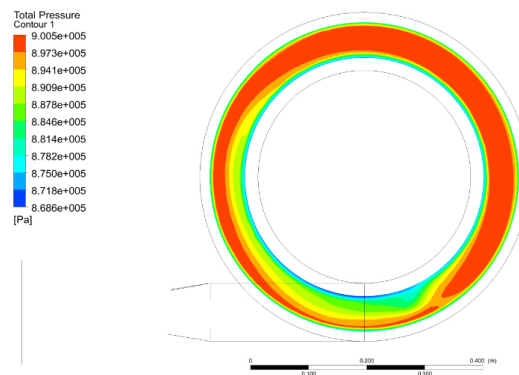


Figure 6: Total pressure in tapering ring, variant 2.

mass flow as well as the velocity in the inlet, which in turn increased the pressure drop. The pressure drop in the inlet was 6.55 kPa and therefore higher than in variant 1.

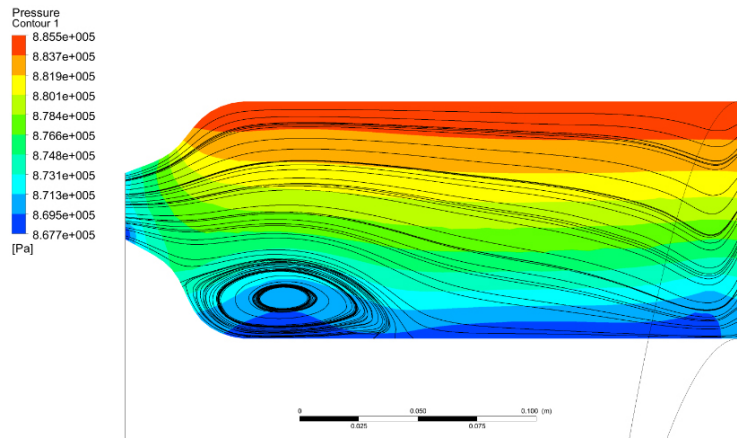


Figure 7: Pressure and streamlines in radial cross-section of variant 2 inlet spiral.

With the new stator profile, the flow in the stator region was not perpendicular to the pressure side of the stator blade (Fig. 8). Changing the first stator profile increased the efficiency from 86.17% to 86.9% and allowed for the steam to flow more in parallel to the pressure side. The turbine power was 1.516 MW and the mass flow was 10.73 kg/s (38.64 t/h). The efficiency was 86.9%.

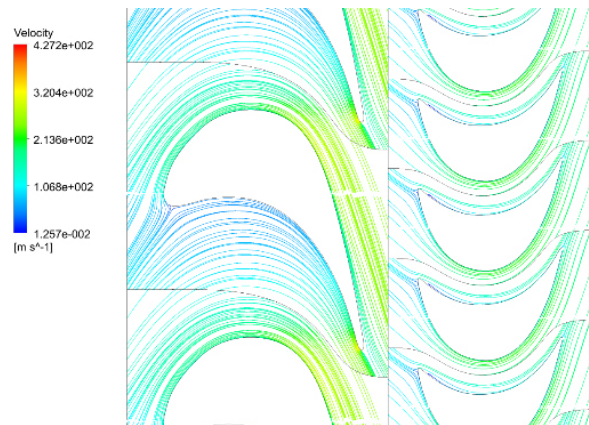


Figure 8: Velocity field in 0.5 length stator blade, variant 2.

### 2.3 Variant 3

In variant 3 the tapering ring was not applied. The wall between the initial channel and ending of spiral (Fig. 1b) was removed and the circular inlet pipe was now fully connected to the spiral (Fig. 9). In contrast to inlet geometry analysed in Sections 2.1 and 2.2, where the initial channel was connected at a slight angle to the spiral, here the initial channel was connected to the spiral perpendicularly to the turbine axis. The profile of the first stator was S-9012A [14] and the number of stators was 32. As in variants 1 and 2, the flow was perpendicular to the pressure side of the first stage stator blades and the angle of attack is below  $90^\circ$ .

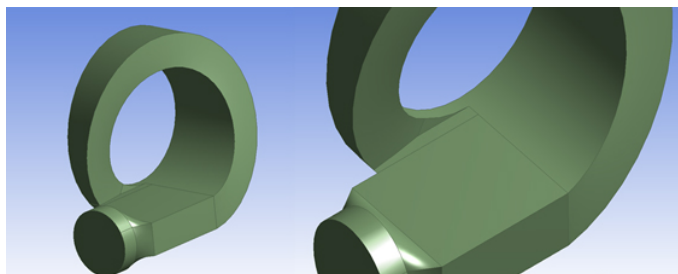


Figure 9: The geometry of the turbine inlet, variant 3.

Despite the connection between the inlet pipe and spiral ending, the flow at the entrance to the first stator row was not uniform. Figure 10 shows

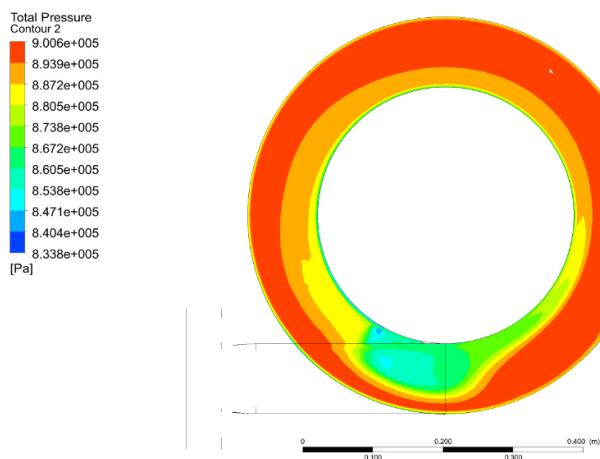


Figure 10: Total pressure near the first stage of turbine, variant 3.

that there is a region of lower values of total pressure near the ending of the spiral. At about 50 kPa, the maximal difference of total pressure is even higher than in variants 1 and 2.

As in variant 1, here entropy distribution was calculated to identify the most important local losses (Fig. 11). The highest entropy value occurs in the connection between the inlet pipe and spiral ending. As in variant 1, other high values appear near the inner surface of the spiral. Figure 12 shows

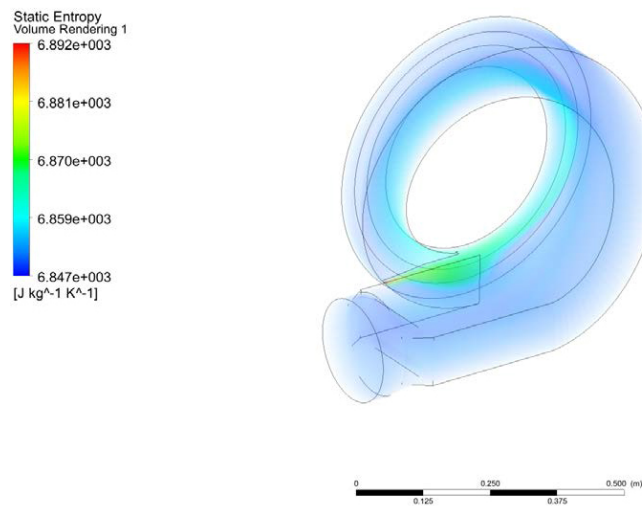


Figure 11: Entropy in inlet geometry, variant 3.

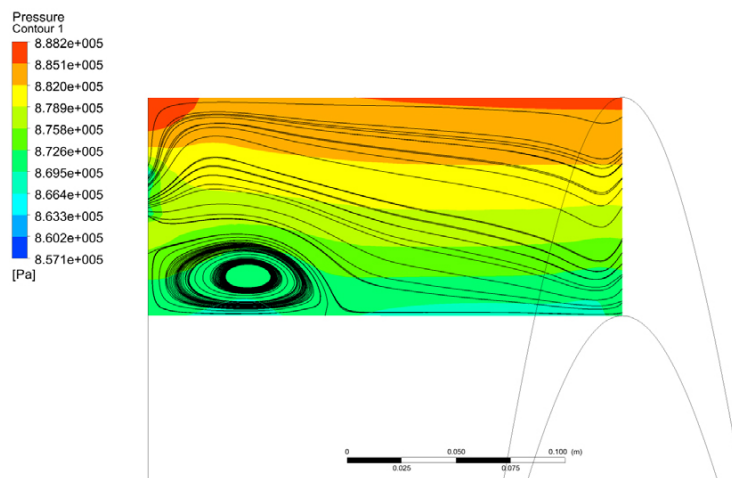


Figure 12: Pressure and streamlines in radial cross section of inlet spiral of variant 3.

that the vortex in this case is more intensive and has a larger diameter, due to lack of tapering. In order to enter the first stage, the flow must turn rapidly, which causes vortices around the first stage stator blade root and tip. The pressure drop in the inlet was 21.15 kPa and was higher than in variants 1 and 2.

As in variant 1, here the S-9012A first stage stator profile was used. This again resulted in a flow perpendicular to the pressure side of first stage stator blades (Fig. 13). The higher pressure drop in the inlet worsened the influx at the roots and even more at the tips of the stators (Fig. 14), resulting in lower turbine efficiency, which was reduced to 83.7%. The turbine power was 1.293 MW and the mass flow was 9.50 kg/s (34.21 t/h).

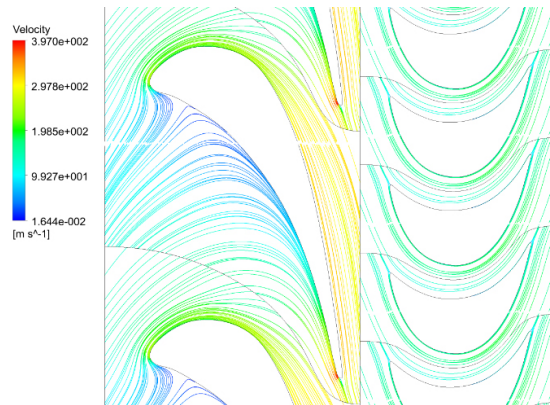


Figure 13: Velocity field in 0.5 length stator blade, variant 3.

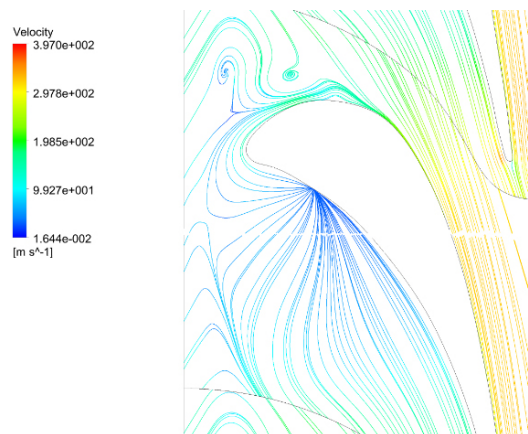


Figure 14: Velocity field in 0.9 length stator blade, variant 3.

## 2.4 Variant 4

The inlet geometry of variant 4 was the same as in variant 3. The profile of the first stator (S-5515A [14]) was changed to prevent the perpendicular flow on the pressure side of first stage stator (Fig. 15). The number of stator blades was increased to 39. However, vortices still appeared around the stator blade tip and root regions due to the rapid change of flow direction out of the inlet. The turbine power was 1.458 MW and mass flow was 10.49 kg/s (37.75 t/h). The pressure drop at the inlet was 24.49 kPa and higher than in variant 3 as a result of higher mass flow. Changing the stator profile in variant 4 increased the turbine efficiency from 83.7% to 85.69%. Similar changes appeared in variant 2 in contrast to variant 1.

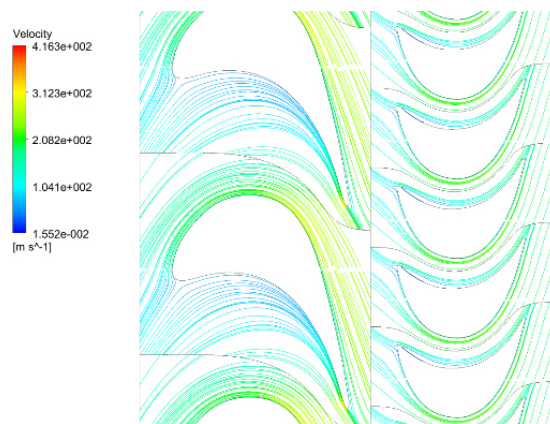


Figure 15: The velocity field in 0.5 length stator blade, variant 4.

## 2.5 Variant 5

The inlet spiral in variant 5 caused the flow almost parallel to the pressure and suction sides of the stator blades and the angle of attack was above  $90^\circ$ . The spiral geometry is shown in Fig. 16. The profile of the first stator (S-9012A [14]) was shortened from 0.0625 m to 0.056 m and the number of stators was 32. The stator blades in other stages were the same as in variants 1 to 4.

The total pressure distribution near the entrance to the first stage in variant 5 is shown in Fig. 17. The maximal circumferential difference in pressure is about 50 kPa. The streamlines in the inlet geometry were slightly changed (Fig. 18). Turbine power was 1.373 MW and the mass flow 9.68 kg/s

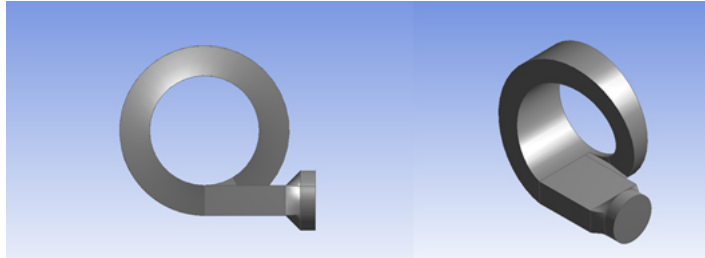


Figure 16: Geometry of the turbine inlet, variant 5.

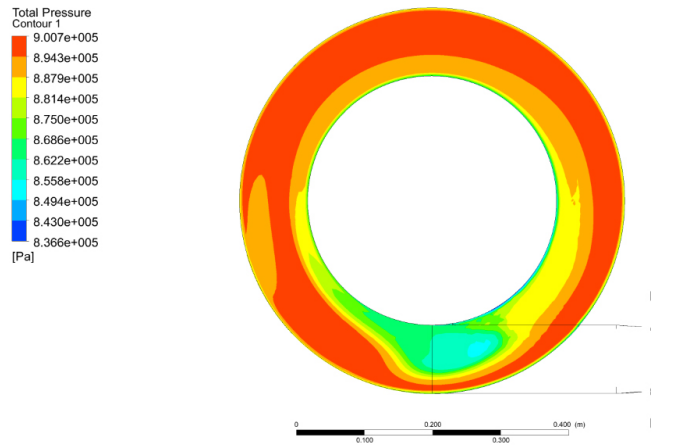


Figure 17: Total pressure near the first stage of turbine, variant 5.

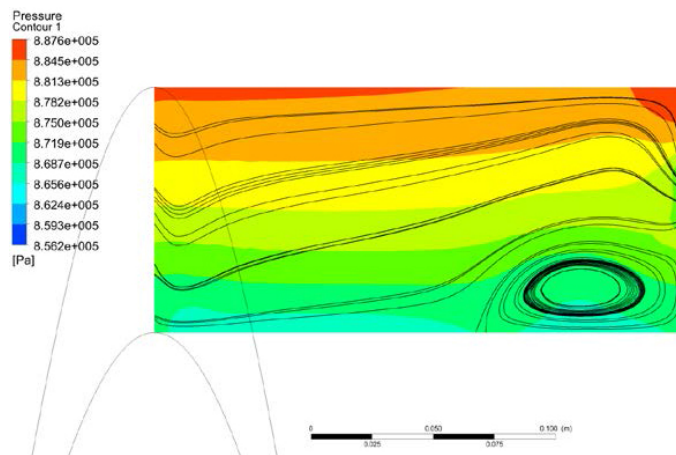


Figure 18: Pressure and streamlines in radial cross-section of inlet spiral, variant 5.

(34.86 t/h). The pressure drop in the inlet was 20.99 kPa. Changing the inlet in variant 5 increased the turbine efficiency from 85.7% to 87.3% due to the flow being more parallel to the pressure and suction of the stator blades Fig. 19.

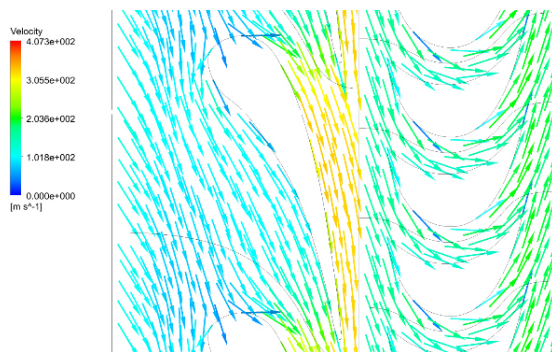


Figure 19: Velocity field in 0.5 length stator blade, variant 5.

## 2.6 Variant 6

In this case, in contrast to variants 1–5, two inlet pipes were used instead of one. The reason for this configuration was to split the admission mass flow as in [11]. Also changed were the connections between the spirals and inlet pipes (Fig. 20). Also in contrast to the previous cases, where the steam flowed out near the middle of spiral, here the steam flowed out near the inner surface of the spiral. The stator blades were the same as in variant 5.

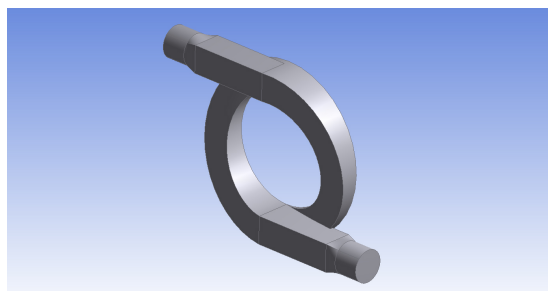


Figure 20: Geometry of the turbine inlet, variant 6.

Figure 21 shows that the distribution of total pressure in this inlet is axisymmetric and nearly uniform. The maximal difference in total pressure values is about 10 kPa, and such differences occur only pointwise.

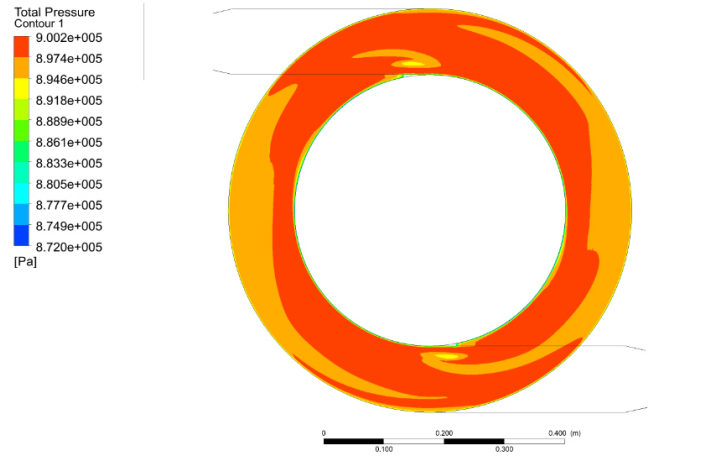


Figure 21: Total pressure near the first stage, variant 6.

The major regions of high entropy in this case occurred on outer surface of the spirals (Fig. 23). The lack of high entropy values in regions where the spirals were connected to the inlet pipes means that this solution is optimal and allows for the minimization of losses. Figure 23 shows that the regions of high entropy in Fig. 22 are vortices. In this case, the vortices

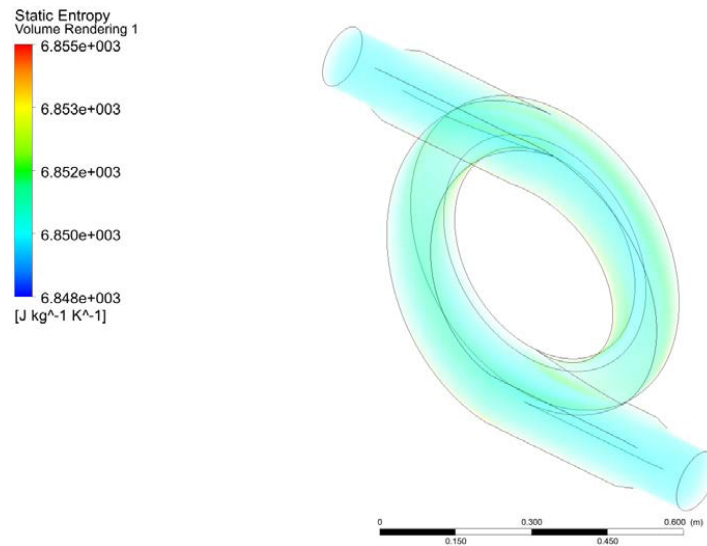


Figure 22: Entropy in inlet geometry, variant 6.

occur further away from the first stage than in the previous variants. It would probably be possible to prevent the vortices from forming in this case, if an additional oblique wall were to be added to the inlet.

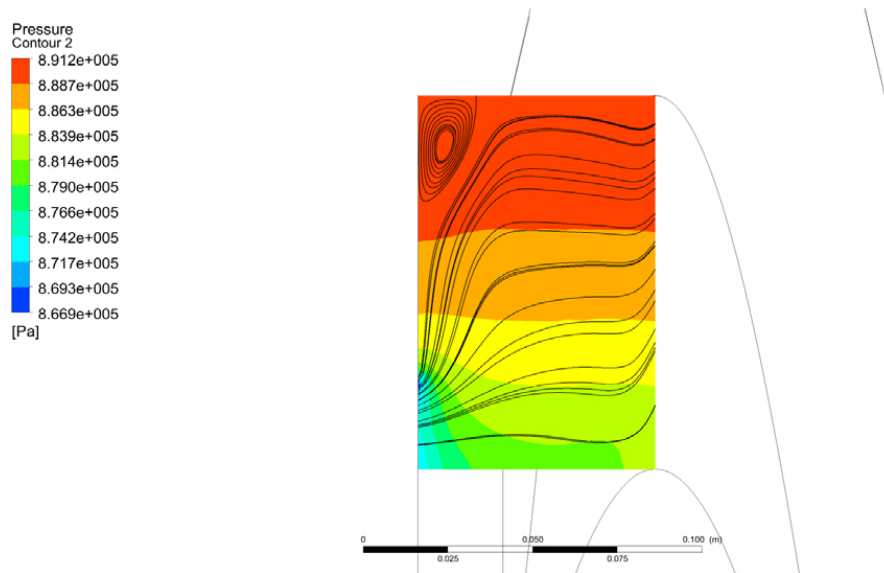


Figure 23: Pressure and streamlines in radial cross-section of inlet spiral, variant 6.

The turbine power was 1.178 MW and the mass flow was 8.21 kg/s (29.31 t/h). The pressure drop in the inlet was 1.24 kPa and considerably smaller than in variants 1 to 5. Changing the inlet geometry in variant 6 increased turbine efficiency from 87.3% to 88.87%. The introduction of two pipes in the inlet results in a higher efficiency and smaller pressure drop in the inlet and is therefore recommended for 1 MW steam turbines. In this case, there was no tapering channel outlet to the stator blades as in variant 1. There was also no wall between inlet pipe and inlet spiral. The spiral with two inlet pipes did not direct the flow perpendicularly to the first stator blade pressure sides. They increased turbine efficiency and decreased the pressure drop. There was no boundary layer separation in the turbine flow in (Fig. 24). Therefore, this variant is recommended for 1 MW steam turbine inlet.

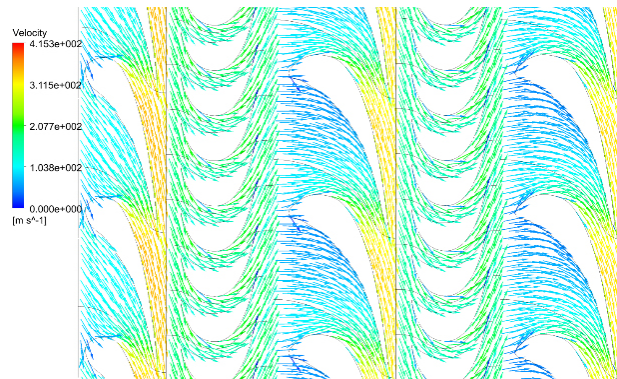


Figure 24: Velocity field in 0.5 length stator blade, variant 6.

## 2.7 Variant 7

In this case, the outlet of the turbine was included to show the basic turbine parameters. Variant 7 had the same inlet as variant 6 and three stages, but also an outlet (Fig. 25). The profile of the 1st stator was modified S-9012A [14]. The turbine power was 1.1 MW and the mass flow was equal to 7.99 kg/s (28.76 t/h). The pressure drop in the inlet was 1.18 kPa even lower than in variant 6 because of the lower mass flow. The calculations of the steady flow that included the outlet showed that the efficiency is generally lower than in the simpler models and it was 85.31%. However the optimal case with the highest efficiency is still the variant 6. The flow velocity in the turbine stages is shown in Fig. 26. As in variant 6, there was no boundary layer separation. The outlet area caused the flow to whirl in many places (Fig. 27), which decreased the turbine efficiency. A flow optimization of the outlet is necessary.

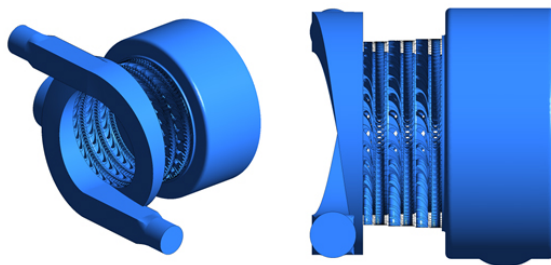


Figure 25: Geometry of the turbine inlet, 3 stages and outlet, variant 7.

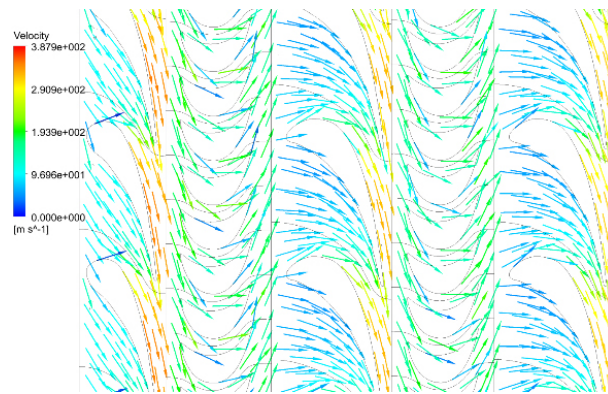


Figure 26: Velocity field in 0.5 length stator blade, variant 7.

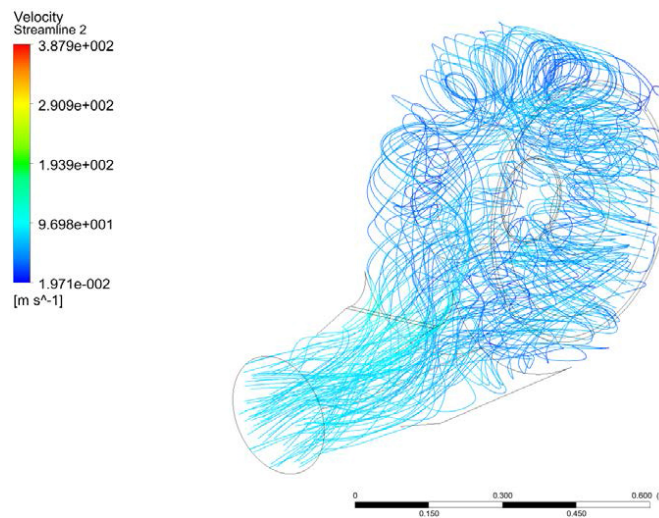


Figure 27: Streamlines in outlet.

### 3 Summary

Several small turbine inlets were analysed. Single-pipe and two-pipe inlets are analysed aerodynamically for the first time, taking into account the stator and rotor blades in three stages to find the best variant. The geometries of the inlets and stator blades were changed to obtain the maximal turbine efficiency. Also analysed for the first time is the occurrence of vortices in the inlets of the studied variants 1–7. Table 1 provides a general description of the inlet geometries presented in this paper.

Table 1: Inlet geometry.

Variant	Tapering	Inlet pipe-spiral connection	90° angle of attack	Position of flow to turbine first stage	Two inlet pipes	Pressure drop in inlet, kPa	Turbine efficiency, %
1	yes	wall at inlet pipe-spiral connection	below	middle	no	5.64	86.17
2	yes	wall at inlet pipe-spiral connection	below	middle	no	6.55	86.90
3	no	no wall	below	middle	no	21.15	83.70
4	no	no wall	below	middle	no	24.49	85.69
5	no	no wall	above	middle	no	20.99	87.30
6	no	both ends of spiral connected to inlet pipes	above	inner surface	yes	1.24	88.87

In variant 1, a circular inlet pipe was connected to the rectangular spiral channel at a slight angle for a smoother flow. The spiral outlet was in the form of a narrowing diffuser leading to the stator blades. The rectangular channel was separated from the ending of the spiral by a wall. The inlet spiral directed the flow at a less than 90° angle of attack in relation to the first stator blades. A stall flow region was visible in the inlet pipe area and spiral and in the stator blades. The velocity was perpendicular to the pressure side, which reduced efficiency to 86.17%. The turbine power was 1.368 MW and the mass flow was 9.78 kg/s (35.21 t/h). The pressure drop in the inlet was 5.64 kPa as the result of converging ring.

Variant 2 had the same inlet spiral geometry as variant 1, but a different 1st stator profile was introduced to change the flow direction, and a number of stator blades was increased to 39 on account of the changed stator profile. With the profile change, the flow in stator region did not stall and the velocity vector was not perpendicular to the pressure side. The inlet spiral caused a reversal of the flow direction in the first stator blades. The turbine power was 1.516 MW and mass flow respectively was 10.73 kg/s (38.64 t/h). The efficiency was 86.9%. The pressure drop in the inlet was 6.55 kPa and was higher than in variant 1 as a result of higher velocity and mass flow. Changing the 1st stator profile in variant 2 increased the efficiency from 86.17% to 86.9% and allowed for the steam to flow in the stator without stalling.

In variant 3, a tapering ring was not applied. The wall between the initial channel and ending of spiral was replaced by a connection between them. The pressure drop in the inlet was 21.15 kPa and was higher than in variants 1 and 2. The efficiency in this case was 83.7%. The turbine power was 1.293 MW and the mass flow was 9.50 kg/s (34.21 t/h).

The inlet geometry of variant 4 was the same as in variant 3. The only change was the profile of the first stator (S-5515A [14]). The number of stator blades was increased to 39. The turbine power was 1.458 MW and the mass flow 10.49 kg/s (37.75 t/h). The pressure drop in the inlet was 24.49 kPa and was higher than in variant 3 as a result of higher mass flow. Changing the stator profile in variant 4 increased the turbine efficiency from 83.7% to 85.69%. A similar change appeared in variant 2 in relation to variant 1.

The inlet spiral in variant 5 directed the flow at a higher than 90° angle of attack in relation to the 1st stage stator blades. In all the previous variants, the angle of attack was below 90°. The profile of the first stator (S-9012A) was shortened from 0.0625 m to 0.056 m and the number of stators was 32. The stator blades in other stages were the same as in variants 1 to 4. The turbine power was 1.373 MW and the mass flow 9.68 kg/s (34.86 t/h). The pressure drop in the inlet was 20.99 kPa. Changing the inlet in variant 5 increased the turbine efficiency from 85.7% to 87.3% as a result of the flow angle of attack being above 90°.

In variant 6, in contrast to variants 1–5, two inlet pipes were used instead of one. The reason for this was to split the mass flow. The turbine power was 1.178 MW and the mass flow 8.21 kg/s (29.31 t/h). The pressure drop in the inlet was 1.24 kPa and was considerably smaller than in the variants 1 to 5. Changing the geometry of the inlet in variant 6 increased the turbine efficiency from 87.3% to 88.87%. The use of two pipes in the inlet resulted in higher efficiency and a smaller pressure drop in the inlet, which suggests that it is optimal for 1 MW steam turbines. In this case there is no outlet in the form of tapering the channel leading the steam to the stator blades as in variant 1.

In variants 1–5, vortices occurred in the region of connection between the spiral and the inlet pipe. In variant 6, these vortices were eliminated. A possible reason for this was the removal of the inlet pipe-spiral connection wall and the gap it created. The flow from the inlet pipe was now smoothly connected with the spiral. Additional analyses should be carried out in order to determine the exact impact of the inlet pipe-spiral connection on turbine efficiency. The rectangular cross-section spiral causes vortices. In

variants 1–5, these vortices appeared on the inner surface of the spiral due to centrifugal forces, but in variant 6 the vortices occurred on the outer surface because the higher inner diameter of the spiral caused the outflow to be level with the first stage. The application of an oblique wall could possibly prevent vortices from forming in variant 6. The vortices were an important part of energy losses in the inlet of variants 1–5. The tapering channel presented in variants 1 and 2 did not prevent the vortices from forming, but it did lower the pressure drop. It also ensured the smooth flow into the first stage, but such a solution increases the length of the turbine, which is a disadvantage in small steam turbines.

The most uniform distribution of pressure in front of the first stage was obtained when the spiral had two inlet pipes. However, further analyses need to be done in order to indicate whether the similar level of uniformity can be obtained with a single inlet pipe, because the losses due to inlet pipe-spiral inlet connection could be a significant factor. It is worth noting that the first stage stator blade profiles had a barely noticeable influence on the distribution of pressure in front of the first stage. This leads to the conclusion that the turbine stages have little effect on the distribution of pressure in the inlet spiral.

**Acknowledgement** The authors wish to acknowledge NCBiR for the financial support of this work (POIR.04.01.04-00-0116/17).

*Received 13 August 2020*

## References

- [1] BELLUCCI J., RUBECHIN F., ARNONE A.: *Modeling partial admission in control stages of small steam turbines with CFD*. In: Proc. ASME Turbo Expo, June 11-15 2018 Oslo, GT2018-76528, 2018.
- [2] LAMPART P., SZYMANIAK M., RZADKOWSKI R.: *Unsteady load of partial admission control stage rotor of a large power steam turbine*. In: Proc. ASME Turbo EXPO 2004, Power for Land, Sea and Air, June 14–17, 2004, Vienna, ASME GT-2004-53886, 2004.
- [3] VAN DEN BRAEMBUSSCHE R.A.: *Flow and loss mechanisms in volutes of centrifugal pumps*. Educational Notes. In: Design and Analysis of High Speed Pumps (12-1–12-26). Educational Notes RTO-EN-AVT-143, Neuilly-sur-Seine, RTO, 2006 (available from: <http://www.rto.nato.int/abstracts.asp>).
- [4] DREXLER C.: *Strömungsvorgänge und Verlustanteile in ungleichförmig beaufschlagten Turbinenstufen*. PhD thesis, RWTH Aachen University, Aachen 1996.

- [5] TRAUPEL W.: *Thermische Turbomaschinen* (4th Edn.). Springer, 2001.
- [6] KOVATS A.: *Effect of non-rotating passages on performance of centrifugal pumps and subsonic compressors*. In: Proc. Winter Annual Meeting, New York 1979.
- [7] LÜDTKE K.: *Centrifugal process compressors – radial vs. tangential suction nozzles*. In: ASME Paper 85-GT-80, 1985.
- [8] SIEVERT R.: *Analyse der Einflussparameter auf die Strömung im Eintritt von Niederdruck-Dampfturbinen*. PhD thesis, Ruhr-Universität Bochum, Bochum 2006 (in German).
- [9] MAIER W.: *Inlet casing for a turbine*. US Patent US5927943A, 1999.
- [10] ŠKACH R., UHER J.: *Spiral Inlets for Steam Turbines*. AIP Conf. Proc. 1889, 020038, 2017.
- [11] HECKER S., ROHE A., STOFF H.: *Steam turbine inlet geometry from a structural and fluid dynamics point of view*. In: Proc. ASME Turbo Expo 2012, GT2012-68678, 2012, 487–495.
- [12] GAO K., WANG C., XIE Y., ZHANG D.: *Effects of inlet chamber structure of the control stage on the unsteady aerodynamic force*. In: Proc. ASME Turbo Expo, Oslo, June 11–15 2018, GT2018-76632, 2018.
- [13] ENGELMANN D., SCHRAM A., POLKLAS T., MAILCH P.: *Losses of steam admission in industrial steam turbines depending on geometrical parameters*. In: Proc. ASME Turbo Expo, Dusseldorf – Oslo, June 16-20 2014, GT2014-25172, 2014.
- [14] DEJCH M.,E., FILIPPOV G.A., LAZAREV L.JA.: *Collection of Profiles for Axial Turbine Cascades*. Machinostroenie, Moscow 1965 (in Russian).
- [15] KIETLIŃSKI K., CZERWIŃSKI P.: *Retrofit of 18K370 steam turbine on the units 7–12 at Belchatow Power Plant*. Arch. Energ. **XLI**(2011), 3-4, 77–96.
- [16] Ansys CFX, Release 18.2.
- [17] Ansys Meshing, Release 18.2
- [18] Ansys TurboGrid, Release 18.2
- [19] Ansys DesignModeller, Release 18.2
- [20] Ansys CFX, Release 18.2, CFX documentation. Ansys, Inc.